

# Hydrophobically modified nanocomposite hydrogels with self-healing ability

Ozge Akca, Berkant Yetiskin, Oguz Okay 

Department of Chemistry, Istanbul Technical University, 34469 Maslak, Istanbul, Turkey

Correspondence to: O. Okay (E-mail: okayo@itu.edu.tr)

**ABSTRACT:** Several strategies have been developed in the past two decades to increase the mechanical performance of the hydrogels, and to generate self-healing function within the polymer network. Here, we combine two of these strategies to create hydrophobically modified nanocomposite (NC) hydrogels with high mechanical strength and self-healing efficiency. The hydrogels were prepared by *in situ* copolymerization of *N,N*-dimethylacrylamide and *n*-octadecyl acrylate (C18A) in the presence of 2 w/v % Laponite clay nanoparticles in an aqueous solution of worm-like sodium dodecyl sulfate micelles. Incorporation of hydrophobic C18A segments into the gel network significantly increases both the storage and loss moduli of NC hydrogels indicating increasing elasticity and energy dissipation. An improvement in the mechanical performance and self-recoverability of NC hydrogels was also observed after hydrophobic modification. The compressive fracture stress and Young's modulus increase with increasing amount of C18A, and they become  $9 \pm 1$  MPa and  $30 \pm 2$  kPa, respectively, at 4 mol % C18A. Incorporation of hydrophobic segments also provides a larger energy dissipation under large strain as compared to the traditional NC hydrogels providing a self-healing efficiency of  $90 \pm 10\%$  in mechanically strong NC hydrogels. © 2019 Wiley Periodicals, Inc. *J. Appl. Polym. Sci.* **2020**, *137*, 48853.

**KEYWORDS:** clay; gels; mechanical properties; micelles; nanoparticles; nanowires and nanocrystals

Received 27 September 2019; accepted 9 December 2019

DOI: 10.1002/app.48853

## INTRODUCTION

Hydrogels are chemically and/or physically crosslinked polymer chains retaining a significant amount of water without dissolving.<sup>1</sup> They attracted significant interest in the past 70 years due to their smartness, and similarity to biological tissues opening a variety of application areas including soft contact lenses, superabsorbent materials, biomaterials, biosensors, and scaffolds for tissue engineering.<sup>2</sup> One drawback in the use of chemically crosslinked hydrogels for load-bearing applications is their brittle nature due to the absence of an energy dissipation mechanism.<sup>3–5</sup> In the past two decades, several techniques have been developed to prepare high strength and tough hydrogels by creating an effective energy dissipation via sacrificial or reversible bonds, including double-network hydrogels,<sup>6–8</sup> topological hydrogels,<sup>9,10</sup> and nanocomposite (NC) hydrogels.<sup>11</sup> NC hydrogels developed by Haraguchi and coworkers were synthesized by *in situ* polymerization of a hydrophilic monomer such as *N,N*-dimethylacrylamide (DMAA) or *N*-isopropylacrylamide (NIPAM) in an aqueous dispersion of Laponite nanoparticles.<sup>11–14</sup> Laponite is a synthetic hectorite clay that forms disk-like particles in water with a thickness and diameter of about 1 and 25 nm, respectively, due to the stabilization effect of their negative surface charge density. Polymerization of DMAA or NIPAM in aqueous Laponite dispersions leads to the

formation of water-stable, highly stretchable hydrogels due to the action of clay nanoparticles as dynamic multifunctional crosslinks with large effective functionality.<sup>11,15–19</sup> Similar to the polymers such as polypropylene reinforced by nanoparticles,<sup>20–23</sup> increasing amount of Laponite also increases the mechanical strength and toughness of NC hydrogels.

Self-healing is a property defining the capability of a material to repair damage autonomously or under the effect of an external stimulus such as the temperature, pH, and light.<sup>24–27</sup> This behavior is, in fact, a naturally occurring phenomenon observed in living beings to survive and grow during their evolutions in billions of years. In the past years, intrinsic and extrinsic self-healing mechanisms have been created in synthetic materials using a wide range of strategies.<sup>28–30</sup> However, the intrinsic mechanism generated using reversible covalent or noncovalent bonds has generally been preferred because the resulting materials can be healed several times when damage occurs at the same location. Intrinsically self-healable polymers or hydrogels were mainly prepared via noncovalent intermolecular interactions such as ionic, hydrophobic, or hydrogen bonding interactions.<sup>31</sup> Among them, hydrophobic interactions created by the incorporation of hydrophobic segments into hydrophilic polymer chains draw particular attention as these interactions provide the integration of excellent

mechanical performance with a high self-healing efficiency.<sup>32–40</sup> One simple route for the preparation of hydrophobically modified hydrogels with self-healing ability is the micellar copolymerization technique carried out in aqueous solutions of worm-like micelles (WLMs).<sup>35</sup> Micellar copolymerization of hydrophilic monomers such as acrylamide, DMAA, or NIPAM with hydrophobic monomers including *n*-octadecyl acrylate (C18A) in aqueous solutions of worm-like sodium dodecyl sulfate (SDS) micelles leads to self-healing hydrogels with extraordinary mechanical properties. Moreover, NC hydrogels also exhibit self-healing ability at elevated temperatures. Haraguchi *et al* showed that the self-healing efficiency of NC hydrogels decreases as the amount of Laponite is increased.<sup>17</sup> Thus, although increasing Laponite content of NC hydrogels also increases their mechanical strength, their ability to self-heal significantly decreases.

The present work aims to create an efficient self-healing in mechanically strong NC hydrogels by generating additional intermolecular interactions. Because hydrophobic interactions are stronger than hydrogen bonds and can easily be tuned by the size and the amount of the hydrophobes,<sup>36,41</sup> we incorporated hydrophobic C18A segments into NC hydrogel network. For this purpose, we conducted the micellar copolymerization of DMAA and C18A in aqueous solutions of WLMs and Laponite nanoclay particles (Figure 1). To our knowledge, there is only one report on hydrophobically modified NC hydrogels where the effect of Laponite clay on the hydrogel properties was investigated.<sup>42</sup> As will be seen below, increasing the amount of the hydrophobe C18A increases the mechanical performance of NC hydrogels at a fixed Laponite content of 2 w/v %. Moreover, incorporation of hydrophobic segments provides a larger energy dissipation under strain as compared to the traditional NC hydrogels providing a complete self-healing efficiency in mechanically stronger hydrogels.

## EXPERIMENTAL

### Materials

*N,N*-DMAA (Sigma-Aldrich, melting point:  $-40\text{ }^{\circ}\text{C}$ ) was purified by filtering through  $\text{Al}_2\text{O}_3$  column to remove the hydroquinone inhibitor. The synthetic hectorite clay Laponite XLG,  $[\text{Mg}_{5.34}\text{Li}_{0.66}\text{Si}_8\text{O}_{20}(\text{OH})_4] \text{Na}_{0.66}$  (Rockwood Ltd), *n*-octadecyl acrylate (C18A, Sigma-Aldrich, melting point:  $32\text{--}34\text{ }^{\circ}\text{C}$ ), ammonium persulfate (APS, Sigma-

Aldrich), *N,N,N',N'*-tetramethylethylenediamine (TEMED, Sigma-Aldrich), SDS (Merck), and sodium chloride (NaCl, Merck) were used without further purification. A stock solution of 8 w/v % APS in distilled water was used in the hydrogel preparation.

### Preparation of Hydrogels

Hydrophobically modified NC hydrogels were prepared via micellar polymerization technique at a total monomer (DMAA + C18A) concentration of 10 w/v % in the presence of 2 w/v % Laponite nanoparticles. The concentrations of SDS, APS, and TEMED at the gel preparation were fixed at 7 w/v %, 3.51 mM, and 0.073 v/v %, respectively. The amount of the hydrophobic monomer C18A in the monomer mixture was varied between 1 and 4 mol% with respect to DMAA. Because C18A was insoluble in SDS solutions, NaCl (0.5 M) was included in the reaction system to create wormlike SDS micelles providing solubilization of C18A in the micellar solution.<sup>35,36,43</sup> Typically, to prepare hydrogels with 1 mol% C18A, SDS (0.70 g) was first dissolved in 0.5 M NaCl solution (4.95 mL) at  $35\text{ }^{\circ}\text{C}$  under stirring for about 1 h. C18A (31.7 mg) was then dissolved in this transparent micellar solution under stirring for 3 h. Separately, DMAA (1.0 mL) was added to a solution of Laponite (0.20 g) in nitrogen-gas bubbled distilled water (3.95 mL) at  $4\text{ }^{\circ}\text{C}$ . The DMAA–Laponite solution was then slowly added to the micellar solution of C18A and stirred until obtaining a transparent solution. After the addition of APS stock solution (0.10 mL) and TEMED (8  $\mu\text{L}$ ) as the initiator and accelerator, respectively, the reaction solution of 10 mL in volume was transferred into plastic syringes of 4.5 mm in internal diameter to conduct the gelation reactions at  $23 \pm 2\text{ }^{\circ}\text{C}$ . To highlight the effect of the hydrophobic monomer C18A on the hydrogel properties, a reference NC hydrogel in the absence of C18A was also prepared in aqueous 2 w/v % Laponite solution at the same monomer concentration.

### Characterization of Hydrogels

Rheological measurements were carried out using a temperature controlled Gemini 150 rheometer system (Bohlin Instruments) with a cone-and-plate geometry (cone angle =  $4^{\circ}$ , diameter = 40 mm). Hydrogel samples subjected to the measurements were prepared between the cone and plate of the rheometer at a gap distance of 150  $\mu\text{m}$ . A water trap was used during the measurements in order to eliminate water evaporation. After the storage modulus  $G'$  of the reaction system attains a plateau value which required about

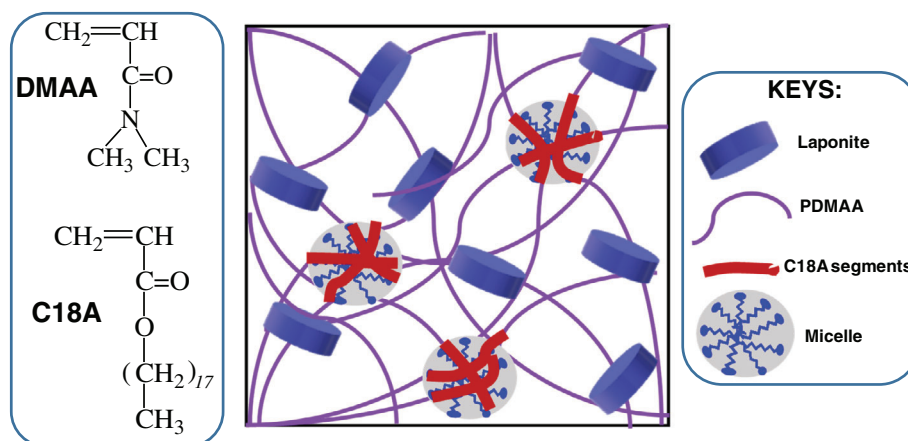


**Figure 1.** Chemical structures of DMAA and C18A monomers, and a cartoon showing the network structure of hydrophobically modified NC hydrogels. [Color figure can be viewed at [wileyonlinelibrary.com](http://wileyonlinelibrary.com)]

30–60 min depending on the C18A content, frequency ( $\omega$ ) sweep tests at 25 °C were carried out at a strain amplitude  $\gamma_0$  of 1%, which was in the linear regime of the hydrogels.

Uniaxial compression tests were carried out at  $23 \pm 2$  °C on a Zwick Roell universal test machine equipped with a 500 N load cell. The tests were performed at a strain rate of  $5 \text{ min}^{-1}$  on cylindrical gel specimens of about 4.5 mm in diameter and  $3.0 \pm 0.3$  mm in length. The nominal stress  $\sigma_{\text{nom}}$  and the strain  $\varepsilon$ , that is, the length change of the sample with respect to its initial length were recorded. The fracture stress  $\sigma_f$  was determined from the maxima of true stress–strain curves, as detailed before.<sup>44</sup> Young's modulus  $E$  was calculated from the slope of  $\sigma_{\text{nom}} - \varepsilon$  curves between 5 and 15% deformation.

Uniaxial tensile tests were also performed using a 500 N load cell at a strain rate of  $5 \text{ min}^{-1}$ . The sample length between jaws was 10 mm. Cyclic tensile tests were conducted at the same strain rate to a maximum strain of 300%, followed by retraction to zero force and a waiting time of 1 min, until the next tensile cycle. To determine the self-healing behavior of the hydrogels, the gel specimens were first cut in the middle and then, the two halves were pressed together within a plastic syringe followed by heating to 50 or 80 °C for 1–5 h, and then cooling to room temperature. Both virgin and healed gel samples were then subjected to tensile tests up to an elongation ratio of 300% to determine the self-healing efficiency. All mechanical tests were conducted on at least five samples for each hydrogel, and the results were averaged.

## RESULTS AND DISCUSSION

Hydrophobically modified NC hydrogels were prepared via micellar copolymerization of DMAA and C18A in the presence of 2 w/v % Laponite nanoparticles. The hydrophobic monomer C18A can easily be dissolved in an aqueous 0.5 M NaCl solution containing 7 w/v % SDS. As reported before,<sup>35,36,43</sup> the presence of NaCl leads to the micellar growth, and the resulting worm-like SDS micelles are able to dissolve a large amount of C18A, during which they undergo a conformation transition from cylindrical to spherical shape (Figure 1). The total monomer (DMAA + C18A) concentration was fixed at 10 w/v % while C18A content in the monomer mixture was varied between 1 and 4 mol% with respect to DMAA.

The rheological properties of the hydrogels were investigated by small strain oscillatory deformation tests at a strain amplitude of 1%. Figure 2

shows frequency ( $\omega$ ) dependencies of the storage modulus  $G'$ , loss modulus  $G''$ , and loss factor  $\tan \delta$  of hydrophobically modified NC hydrogels at various C18A contents as indicated. Without C18A, labeled by "0" in the figures, both  $G'$  and  $\tan \delta$  are almost independent of the frequency  $\omega$ , and  $\tan \delta$  remains at around 0.1. With the addition of C18A, both  $G'$  and  $G''$  increase indicating increasing elastic and viscous characters of NC hydrogels. Moreover,  $G'$  also increases with increasing frequency  $\omega$  approaching a plateau value at high frequencies during which  $\tan \delta$  decreases. This indicates that at a high  $\omega$ , that is, at a short experimental time scale, the number of C18A associations acting as crosslinks increases contributing to the elasticity of the hydrogels.

Mechanical properties of the hydrogels were investigated by uniaxial compression tests at a constant strain rate of  $5 \text{ min}^{-1}$ . Figure 3(a) shows stress–strain curves of hydrophobically modified NC hydrogels at various C18A contents. To highlight the initial slope of the curves, that is, Young's modulus  $E$  of the hydrogels, the insets to the figures show a semilogarithmic presentation of the curves between 0 and 50% strain. The general trend is that the hydrogels sustain around 95% compression and their moduli  $E$  increase with increasing C18A content. This trend is also seen in Figure 3(b) showing the modulus  $E$ , and the fracture stress  $\sigma_f$  of the hydrogels plotted against C18A content. The modulus is  $4.6 \pm 0.4$  kPa in the absence of C18A while it sixfold increases and becomes  $30 \pm 2$  kPa after addition of 4 mol% C18A, revealing that the associations between C18A segments act as additional crosslinks in NC hydrogels. The fracture stress  $\sigma_f$  also increases with increasing C18A content and becomes  $9 \pm 1$  MPa at 4 mol% C18A. The results thus show that, instead of increasing the Laponite content of NC hydrogels, their mechanical performances can also be improved by incorporation of the hydrophobic C18A segments into the PDMAA chains.

The results also show that NC hydrogels with and without C18A sustain high compression ratios due to the dynamic nature of their crosslinks. However, hydrophobic modification also improved the fatigue resistance of the resulting hydrogels. For example, Figure 4(a, b) shows the images of NC hydrogels with and without 4 mol% C18A, respectively, during stretching by hand. The images (i) and (ii) present their stretching up to 1000% strain while the images (iii) were taken from the specimens just after their unloading. A

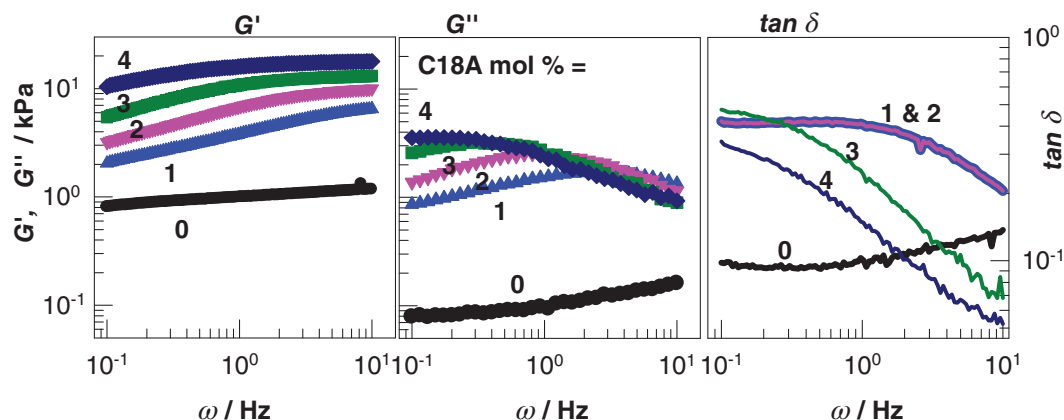


**Figure 2.** Storage modulus  $G'$ , loss modulus  $G''$ , and loss factor  $\tan \delta$  of hydrophobically modified NC hydrogels plotted against the frequency  $\omega$ . Laponite = 2 w/v %. C18A contents are indicated. [Color figure can be viewed at [wileyonlinelibrary.com](http://wileyonlinelibrary.com)]

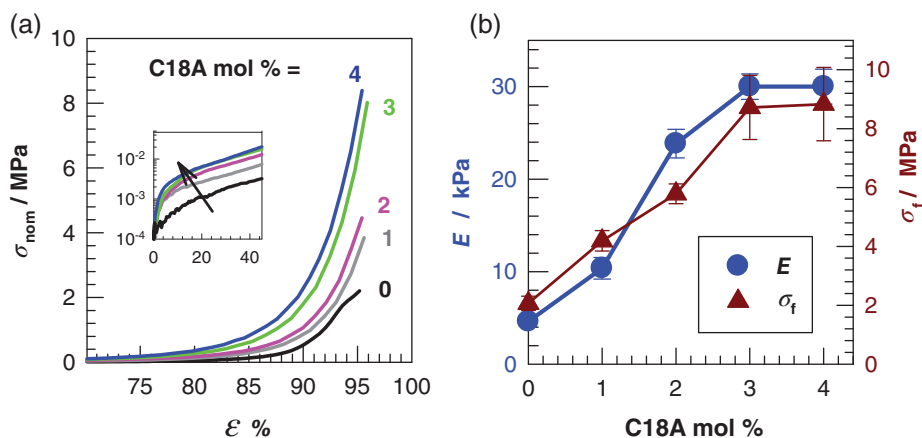


**Figure 3.** (a) Stress–strain curves of hydrophobically modified NC hydrogels. The inset is a semilogarithmic presentation of the curves between 0 and 50% strain. C18A contents are indicated. (b) Young's modulus  $E$  and fracture stress  $\sigma_f$  of the hydrogels plotted against C18A concentration. [Color figure can be viewed at [wileyonlinelibrary.com](http://wileyonlinelibrary.com)]

rapid recovery of hydrophobically modified NC hydrogel close to its initial length is seen as compared to the unmodified one. Moreover, permanent deformation after equilibrium was about 30 and 50% for modified and unmodified hydrogels indicating that the hydrophobic associations contribute to the shape-recovery ability of the hydrogels.

Cyclic mechanical tests are a mean to detect the nature of intermolecular bonds in physical hydrogels. NC hydrogels with and without C18A were subjected to cyclic tensile tests consisting of five successive loading and unloading steps up to a maximum strain of 300% with a waiting time of 1 min between the cycles. Figure 5(a) presents typical cyclic tensile stress–strain curves of a hydrophobically modified NC hydrogel specimen with 3 mol% C18A, where the loading and unloading steps are shown by the solid and dotted curves. The unloading curves follow a different path from the loadings revealing that some intermolecular bonds in the hydrogel are broken during stretching. Moreover, first loading curve significantly deviates from the following loadings indicating that the main damage occurs during stretching of the virgin hydrogel. Similar loading and unloading curves were obtained for all hydrogels despite the fact that they preserve their macroscopic shapes even until 1000% elongation.

The area between the loading and unloading curves, that is, the hysteresis energy  $U_{hys}$  corresponds to the energy dissipated due to the fracture of intermolecular bonds in the hydrogels.  $U_{hys}$  was calculated as,<sup>36</sup>

$$U_{hys} = \int_0^{\epsilon_{max}} \sigma_{nom} d\epsilon - \int_{\epsilon_{max}}^0 \sigma_{nom} d\epsilon \quad (1)$$

where the maximum strain  $\epsilon_{max}$  equals to 3 in our mechanical tests. Moreover, energy dissipation coefficient  $\mu$  indicating the ratio of dissipated to the loading energy per tensile cycle was calculated as,<sup>45</sup>

$$\mu = \frac{U_{hys}}{\int_0^{\epsilon_{max}} \sigma_{nom} d\epsilon} \quad (2)$$

Figure 5(b,c) shows the hysteresis energy  $U_{hys}$ , and energy dissipation coefficients  $\mu$  of NC hydrogels, respectively, prepared without (open symbols) and with 3 mol% C18A (filled symbols). The incorporation of C18A segments into PDMAA chains

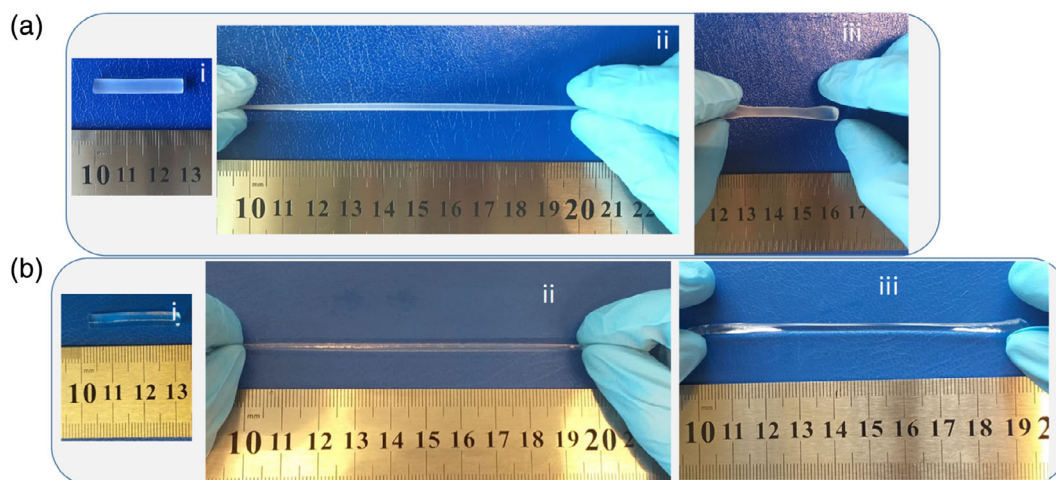


**Figure 4.** Images of NC hydrogels with (a) and without 4 mol% C18A (b) during stretching by hand. The images labeled by (i) and (ii) show their stretching up to 1000% strain. The images (iii) show the specimens just after unloading. [Color figure can be viewed at [wileyonlinelibrary.com](http://wileyonlinelibrary.com)]

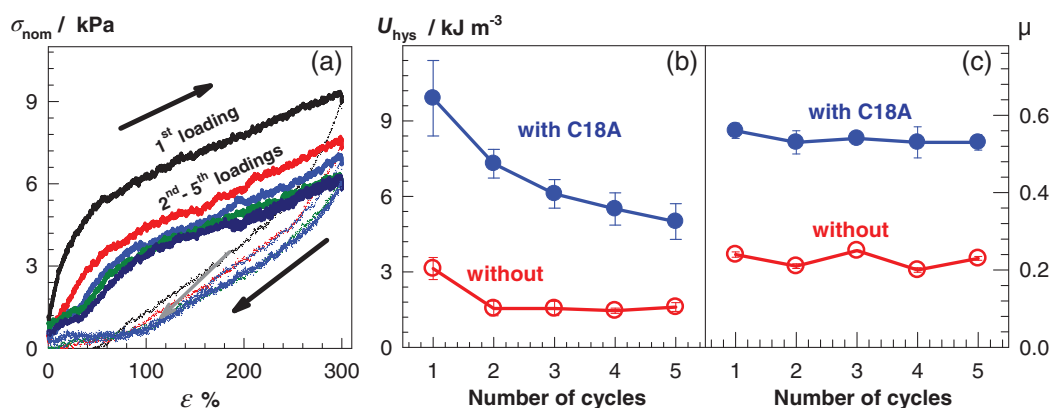


**Figure 5.** (a) Typical cyclic stress–strain curves of a hydrophobically modified NC hydrogel specimen with 3 mol% C18A. Solid and dotted curves represent the loading and unloading curves, respectively. They are also indicated by up and down arrows, respectively. Hysteresis energy  $U_{hys}$  (b), and energy dissipation coefficients  $\mu$  (c) of NC hydrogels without (open symbols) and with 3 mol% C18A (filled symbols) as a function of the number of cycles. [Color figure can be viewed at [wileyonlinelibrary.com](http://wileyonlinelibrary.com)]

significantly increases both the hysteresis energy  $U_{hys}$  and dissipation coefficients  $\mu$ . Because  $U_{hys}$  is proportional to the number of bonds broken during a tensile cycle,<sup>35</sup> larger hysteresis energies reflect larger number of broken physical bonds in hydrophobically modified NC hydrogels as compared to the unmodified ones. This is attributed to the existence of dual intermolecular interactions in hydrophobically modified NC hydrogels, namely, hydrogen bonding interactions between PDMAA and clay surfaces, and hydrophobic interactions between PDMAA chains via C18A segments. The energy dissipation coefficient  $\mu$  of the hydrogels also supports this finding [Figure 6(c)].  $\mu$  of the hydrophobically modified and unmodified NC hydrogels are around 0.5 and 0.2, respectively, revealing that the energy dissipated per loading energy increases from 20 to 50% after hydrophobic modification of PDMAA chains.

Previous works show that NC hydrogels exhibit self-healing ability at elevated temperatures.<sup>17</sup> The efficiency of self-healing was found to decrease with increasing amount of Laponite. For instance, NC hydrogel with 1.1 w/v % Laponite completely heals within 3 h at 50 °C whereas at or above 5.3 w/v % Laponite, a complete healing cannot be achieved. Thus, although increasing Laponite content of NC hydrogels also increases their mechanical strength, their ability to self-heal significantly decreases. In the present work, instead of increasing the Laponite content, we included C18A hydrophobe to improve the mechanical properties. We observed that the self-healing ability of the hydrogels remained unchanged after this modification. For example, Figure 6(a) shows images of a NC hydrogel specimen with 3 mol % C18A before (i), and after cutting into two parts (ii), and after healing at 50 °C for 1 h (iii), and during stretching of the healed hydrogel (iv, v). Similar to the virgin hydrogel, the healed gel specimen can be stretched to around 450% strain by hand. To quantify self-healing, cut-and-heat tests were conducted on hydrogel specimens at both 50 and 80 °C with various healing times between 1 and 5 h. Both virgin and healed specimens were then subjected to uniaxial tensile tests up to an elongation ratio of 300%. Note that the gel specimens were too slippery and no reproducible results could be obtained under larger strain. The

self-healing efficiency  $\eta$  of the hydrogels was quantified using the equation  $\eta = E_H/E_V$ , where  $E_H$  and  $E_V$  are the Young's moduli of healed and virgin specimens, respectively.

Figure 6(b,c) shows the tensile stress–strain curves of virgin and healed NC hydrogels containing 3 mol% C18A. Healing was performed at 50 (b) and 80 °C (c) for 1, 3, and 5 h as indicated in the figures. The gray curves in Figure 6(b) show the stress–strain curves of virgin and healed NC hydrogels without C18A. The stress–strain curves of virgin and healed samples nearly overlap with each other indicating a complete healing of the initial mechanical properties. Indeed, the healing efficiency  $\eta$  at both 50 and 80 °C and after a healing time of 1 h was calculated as  $90 \pm 10\%$  for all hydrophobically modified hydrogels. Thus, the self-healing ability of the hydrophobically modified hydrogels is nearly temperature and healing time independent within the range studied. Although this behavior is similar to the NC hydrogel without C18A, self-healing behavior could be created in a mechanically robust hydrogel after hydrophobic modification.

The self-healing ability of hydrophobically modified NC hydrogels is due to the existence of H-bonding and hydrophobic interactions generating a 3D physical network. It is known that in Laponite/polymer aqueous solutions, many polymer chains attached to the Laponite nanoparticles through H-bonds interconnect them to form a physical network. Thus, Laponite acts as a multifunctional crosslinker during the polymerization of hydrophilic monomers in aqueous solutions. For instance, in NC hydrogels based on polyacrylamide (PAAm), the number of elastically effective network chains per nanoparticle increases from 9 to 180 with increasing Laponite concentration.<sup>15</sup> Moreover, the total number of PAAm chains per nanoparticle is much larger because a considerable fraction of them attach on only one particle and cannot contribute to the rubber elasticity of the hydrogel. The dynamic adsorption and desorption of polymer chains on particle surfaces leads to energy dissipation under strain. In addition to H-bonding interactions, hydrophobic interactions also exist in the present hydrogels due to the presence of mixed micelles composed of hydrophobic C18A segments and SDS

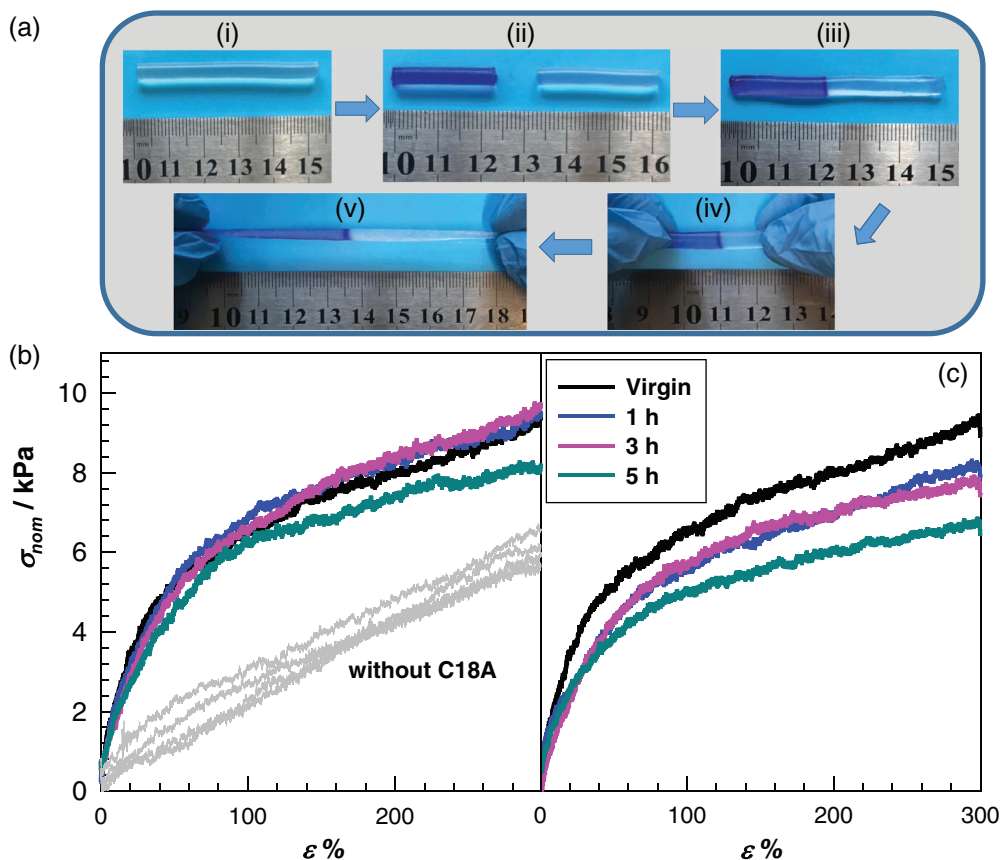


**Figure 6.** (a) Images of a hydrogel specimen with 3 mol% C18A before (i) and after cutting into two parts (ii), after heating at 50 °C for 1 h (iii), and during stretching to 450% strain (iv,v). One of the gel parts is colored with methylene blue for clarity. (b, c) Tensile stress–strain curves of virgin and healed hydrophobically modified NC hydrogels. C18A = 3 mol%. Healing temperature = 50 (b), and 80 °C (c). Gray curves show the data of virgin and healed NC hydrogels prepared without C18A. [Color figure can be viewed at [wileyonlinelibrary.com](http://wileyonlinelibrary.com)]

creating hydrophobic associations between the chains. If a gel specimen is cut into two parts, some H-bonds and mixed micelles are broken at the cut regions, as illustrated schematically in Figure 7. Because the cut surfaces are in contact with air, hydrophobic C18A segments and SDS alkyl groups tend to escape from the water-containing hydrogel phase and orient toward to the cut surface. After bringing the cut surfaces together, broken H-bonds and hydrophobic associations reform between the surfaces and

hence heal the damaged area (Figure 7). This healing process is accelerated with increasing temperature due to the increasing mobility of the polymer chains facilitating the diffusion of polymer chains along the surfaces.

## CONCLUSIONS

Several strategies have been developed in the past two decades to increase the mechanical performance of the hydrogels and to

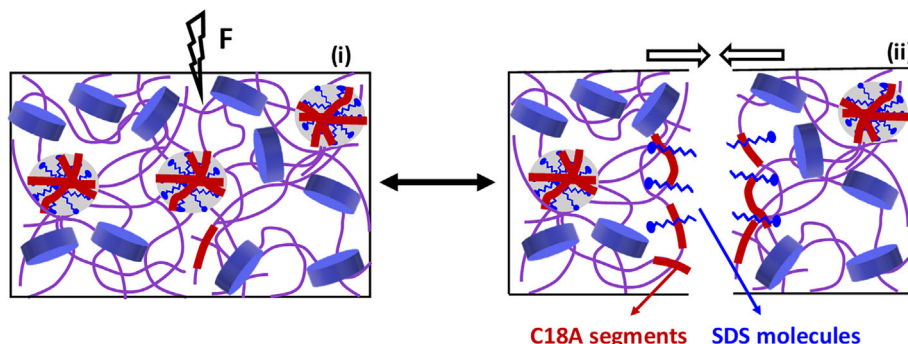


**Figure 7.** Cartoon showing self-healing mechanism of the hydrogels. The images (i) and (ii) show a hydrogel specimen before and after cutting into two parts, respectively (see Figure 1 for explanation of the symbols). [Color figure can be viewed at [wileyonlinelibrary.com](http://wileyonlinelibrary.com)]

generate self-healing within the gel network. Here, we combined two of these strategies in the hydrogel preparation, namely, the *in situ* polymerization of DMAA in aqueous dispersion of Laponite clay nanoparticles, and the micellar polymerization of DMAA in the presence of the hydrophobic monomer C18A to generate hydrophobically modified NC hydrogels. Rheological measurements reveal that the hydrophobic modification of NC hydrogels at a Laponite content of 2 w/v % significantly increases both the storage and loss moduli of NC hydrogels indicating their increasing elastic and viscous characters. An improvement in the mechanical properties and self-recoverability of the hydrogels was also observed upon incorporation of hydrophobic C18A segments into the gel network. The compressive fracture stress and Young's modulus increase with increasing C18A content and they become  $9 \pm 1$  MPa and  $30 \pm 2$  kPa, respectively, at 4 mol% C18A. Moreover, hydrophobic segments in NC hydrogels also create a larger energy dissipation under strain as compared to the traditional NC hydrogels due to the existence of both hydrogen bonding and hydrophobic interactions. The energy dissipated per loading energy increases from 20 to 50% after incorporation of 3 mol% C18A into the PDMAA chains. Moreover, a self-healing efficiency of  $90 \pm 10\%$  with respect to the modulus  $E$  could be generated by healing the damaged hydrogels at  $50^\circ\text{C}$  for 1 hour. Although this behavior is similar to the NC hydrogel without C18A, self-healing behavior could be created in a mechanically robust hydrogel after hydrophobic modification.

#### ACKNOWLEDGMENTS

O.O. thanks the Turkish Academy of Sciences (TUBA) for the partial support.

#### REFERENCES

- Okay, O. *Springer Ser. Chem. Sens. Biosens.* **2009**, 6, 1.
- Calvert, P. *Adv. Mater.* **2009**, 21, 743.
- Ahagon, A.; Gent, A. N. *J. Polym. Sci. Polym. Phys. Ed.* **1975**, 13, 1903.
- Brown, H. R. *Macromolecules.* **2007**, 40, 3815.
- Creton, C. *Macromolecules.* **2017**, 50, 8297.
- Gong, J. P.; Katsuyama, Y.; Kurokawa, T.; Osada, Y. *Adv. Mater.* **2003**, 15, 1155.
- Nakayama, A.; Kakugo, A.; Gong, J. P.; Osada, Y.; Takai, M.; Erata, T.; Kawano, S. *Adv. Funct. Mater.* **2004**, 14, 1124.
- Haque, M. A.; Kurokawa, T.; Gong, J. P. *Polymer.* **2012**, 53, 1805.
- Okumura, Y.; Ito, K. *Adv. Mater.* **2002**, 13, 485.
- Karino, T.; Shibayama, M.; Ito, K. *Phys. B Condens. Matter.* **2006**, 385, 692.
- Haraguchi, K.; Takehisa, T. *Adv. Mater.* **2002**, 14, 1120.
- Haraguchi, K.; Takehisa, T.; Fan, S. *Macromolecules.* **2002**, 35, 10162.
- Haraguchi, K.; Farnworth, R.; Ohbayashi, A.; Takehisa, T. *Macromolecules.* **2003**, 36, 5732.
- Haraguchi, K.; Li, H. J.; Matsuda, K.; Takehisa, T.; Elliott, E. *Macromolecules.* **2005**, 38, 3482.
- Okay, O.; Oppermann, W. *Macromolecules.* **2007**, 40, 3378.
- Kokabi, M.; Sirousazar, M.; Hassan, Z. M. *Eur. Polym. J.* **2007**, 43, 773.
- Haraguchi, K.; Uyama, K.; Tanimoto, H. *Macromol. Rapid Commun.* **2011**, 32, 1253.
- Liu, R.; Liang, S.; Tang, X. Z.; Yan, D.; Li, X.; Yu, Z. Z. *J. Mater. Chem.* **2012**, 22, 14160.
- Zhou, C.; Wu, Q. *Colloids Surf., B.* **2011**, 84, 155.
- Zdiri, K.; Elamri, A.; Hamdaoui, M.; Harzallah, O.; Khenoussi, N.; Brendle, J. *Green Chem. Lett. Rev.* **2018**, 11, 296.
- Zdiri, K.; Harzallah, O.; Elamri, A.; Khenoussi, N.; Brendle, J.; Mohamed, H. *Adv. Polym. Technol.* **2019**, 37, 3759.
- Zdiri, K.; Elamri, A.; Hamdaoui, N.; Harzallah, O.; Khenoussi, N.; Brendle, J. *Waste Biomass Valor.* **2018**. <https://doi.org/10.1007/s12649-018-0427-2>.
- Zdiri, K.; Elamri, A.; Hamdaoui, M.; Khenoussi, N.; Harzallah, O.; Brendle, J. *J. Thermoplast. Compos. Mater.* **2019**, 32, 1159.
- Habault, D.; Zhang, H.; Zhao, Y. *Chem. Soc. Rev.* **2013**, 42, 7244.
- Li, G.; Zhang, H.; Fortin, D.; Fan, W.; Xia, H.; Zhao, Y. *J. Mater. Chem. C.* **2016**, 4, 5932.
- Guo, Z.; Ma, W.; Gu, H.; Feng, Y.; He, Z.; Chen, Q.; Mao, X.; Zhang, J.; Zheng, L. *Soft Matter.* **2017**, 13, 7371.
- Banerjee, S. L.; Bhattacharya, K.; Samanta, S.; Singha, N. K. *ACS Appl. Mater. Interfaces.* **2018**, 10, 27391.
- Hager, M. D.; Greil, P.; Leyens, C.; Van Der Zwaag, S.; Schubert, U. S. *Adv. Mater.* **2010**, 22, 5424.
- Toohy, K. S.; Sottos, N. R.; Lewis, J. A.; Moore, J. S.; White, S. R. *Nat. Mater.* **2007**, 6, 581.
- White, S. R.; Sottos, N. R.; Geubelle, P. H.; Moore, J. S.; Kessler, M. R.; Sriram, S. R.; Brown, E. N.; Viswanathan, S. *Nature.* **2001**, 409, 794.
- Taylor, D. L.; In het Panhuis, M. *Adv. Mater.* **2016**, 28, 9060.
- Abdurrahmanoglu, S.; Can, V.; Okay, O. *Polymer.* **2009**, 50, 5449.
- Miquelard-Garnier, G.; Demeures, S.; Creton, C.; Hourdet, D. *Macromolecules.* **2006**, 39, 8128.
- Abdurrahmanoglu, S.; Cilingir, M.; Okay, O. *Polymer.* **2011**, 52, 694.
- Tuncaboylu, D. C.; Sahin, M.; Argun, A.; Oppermann, W.; Okay, O. *Macromolecules.* **2012**, 45, 1991.
- Tuncaboylu, D. C.; Argun, A.; Sahin, M.; Sari, M.; Okay, O. *Polymer.* **2012**, 53, 5513.
- Akay, G.; Hassan-Raeisi, A.; Tuncaboylu, D. C.; Orakdogan, N.; Abdurrahmanoglu, S.; Oppermann, W.; Okay, O. *Soft Matter.* **2013**, 9, 2254.
- Bilici, C.; Okay, O. *Macromolecules.* **2013**, 46, 3125.

39. Gulyuz, U.; Okay, O. *Soft Matter*. **2013**, *9*, 10287.
40. Argun, A.; Algi, M. P.; Tuncaboylu, D. C.; Okay, O. *Colloid Polym. Sci.* **2014**, *292*, 511.
41. Talebian, S.; Mehrali, M.; Taebnia, N.; Pennisi, C. P.; Kadumudi, F. B.; Foroughi, J.; Hasany, M.; Nikkhah, M.; Akbari, M.; Orive, G. *Adv. Sci.* **2019**, *6*, 1801664.
42. Wang, F.; Yong, X.; Deng, J.; Wu, Y. *RSC Adv.* **2018**, *8*, 16773.
43. Can, V.; Kochovski, Z.; Reiter, V.; Severin, N.; Siebenbürger, M.; Kent, B.; Just, J.; Rabe, J. P.; Ballauff, M.; Okay, O. *Macromolecules*. **2016**, *49*, 2281.
44. Argun, A.; Can, V.; Altun, U.; Okay, O. *Macromolecules*. **2014**, *47*, 6430.
45. Yetiskin, B.; Okay, O. *Int. J. Biol. Macromol.* **2019**, *122*, 1279.